Coded access optical sensor (CAOS) imager and applications

Riza, Nabeel

Nabeel A. Riza, "Coded access optical sensor (CAOS) imager and applications," Proc. SPIE 9896, Optics, Photonics and Digital Technologies for Imaging Applications IV, 98960A (29 April 2016); doi: 10.1117/12.2227699

SPIE.

Event: SPIE Photonics Europe, 2016, Brussels, Belgium

Coded Access Optical Sensor (CAOS) Imager and Applications

Nabeel A. Riza
School of Engineering
University College Cork
College Road, Cork, Ireland

ABSTRACT

Starting in 2001, we proposed and extensively demonstrated (using a DMD: Digital Micromirror Device) an agile pixel Spatial Light Modulator (SLM)-based optical imager based on single pixel photo-detection (also called a single pixel camera) that is suited for operations with both coherent and incoherent light across broad spectral bands. This imager design operates with the agile pixels programmed in a limited SNR operations starring time-multiplexed mode where acquisition of image irradiance (i.e., intensity) data is done one agile pixel at a time across the SLM plane where the incident image radiation is present. Motivated by modern day advances in RF wireless, optical wired communications and electronic signal processing technologies and using our prior-art SLM-based optical imager design, described using a surprisingly simple approach is a new imager design called Coded Access Optical Sensor (CAOS) that has the ability to alleviate some of the key prior imager fundamental limitations. The agile pixel in the CAOS imager can operate in different time-frequency coding modes like Frequency Division Multiple Access (FDMA), Code-Division Multiple Access (CDMA), and Time Division Multiple Access (TDMA). Data from a first CAOS camera demonstration is described along with novel designs of CAOS-based optical instruments for various applications.

1. INTRODUCTION

The ability to "*see*" with application-specific intelligence is critical in today's world of big data that is saturated with diverse image characteristics across fundamental science and industry [1-3]. Depending on the application, imaging systems are called scanners, profilers, cameras, imagers, and optical sensors. Classic state-of-the-art optical imager designs in a variety of applications deploy photo-detector arrays such as the Charge Coupled Devices (CCDs) and the Complementary Metal Oxide Semiconductor (C-MOS) optical sensor devices. So although some high end commercial and research stage CCD/CMOS imagers are indeed showing some excellent emerging merits [4-5], there is still a strong need for alternative design imagers that can operate under extreme lighting contrast conditions (e.g., > 10^4:1) without the use of direct light attenuation and also provide spectrum detection flexibility, e.g., operate in two different spectral bands. In some scenarios, the desired imager should be able to operate with possible object motion and deliver high resolution, high dynamic range, low inter-pixel crosstalk, and high Signal-to-Noise Ratio (SNR) images with minimal motion blur. Plus the imager should be low cost, compact and mechanically robust and be capable of providing data compressed image information.

Starting in 2001, the Riza group proposed and extensively demonstrated (using a DMD: Digital Micromirror Device) an agile pixel Spatial Light Modulator (SLM)-based optical imager based on single pixel and dual pixel photo-detection that is suited for operations with both coherent and incoherent light across broad spectral bands [6-13]. This imager design operates with the agile pixels programmed in a limited SNR operations starring time-multiplexed mode where acquisition of image irradiance (i.e., intensity) data is done one agile pixel at a time across the SLM plane where the desired incident image radiation is present. In effect, the agile pixel electronically adapts in a deterministic way to the imaging scenario to extract the user desired image data. This imager does not use pseudo-random spatial coding of the optical radiation with iterative computational signal processing of the detected photo-current to produce an estimated "*computational*" image. The Riza group imager physically samples and detects the true optical irradiance information and then deploys computer processing to stitch the agile pixel data to produce the user desired image map. This imager can operate adaptively to electronically reprogram its user specified agile pixel settings to improve desired imaged data quality. To put things in context, it is important to note that imaging with a single pixel (or single point detector) goes back to the late 1960's when USSR space program and NASA explored robust imager designs for space missions [14-15]. Today, the Riza group proposed SLM-based agile pixel imager design [6] is being called by some as a single pixel imager/camera (as one point photo-detector can be used for light detection versus a multi-element detector array). This basic imager has been engineered to implement Compressed Sensing (CS) based imaging [16] where the DMD imparts

Optics, Photonics and Digital Technologies for Imaging Applications IV, edited by Peter Schelkens, Touradj Ebrahimi, Gabriel Cristóbal, Frédéric Truchetet, Pasi Saarikko, Proc. of SPIE Vol. 9896, 98960A · © 2016 SPIE · CCC code: 0277-786X/16/$18 · doi: 10.1117/12.2227699

pseudo-random spatial codes on the light irradiance under observation and spatial correlation methods and iterative imaging processing are deployed to create an estimate of the true image that is considered of sparse spatial content. Interesting, essentially the same optical design as the Riza group proposed SLM-based imager has been used to form a ghost computational [17] and ghost compressive imager [18], but in this case, the SLM codes the light before it strikes the object to be imaged. It is also important to note that coding of optical radiation for designing a variety of single photo-detector optical instruments has been around for over 50 years and has been deployed in a variety of ways (moving 2-D binary spatial codes) to extract spectral and spatial information [19-23]. For example, the ref.19 single pixel spectrometer encodes infrared optical spectra with two dimensionally patterned rotating gratings while the ref.23 single pixel active 3-D imager (using a laser) deploys 2-D spatial codes (of CDMA variety) to encode and decode scanned object pixel irradiances in the 3-D sample space.

Motivated by modern day advances in RF wireless, optical wired communications and ultra-high speed electronic signal processing and photonic device technologies and using our prior-art SLM-based imager design [6], described is a new and improved imager design platform called Coded Access Optical Sensor (CAOS) [24, 25] that has the ability to alleviate some of the mentioned prior imager fundamental limitations using a surprisingly simple approach of time-frequency-space coded access using an agile pixel. For example, presented in this paper is a novel hybrid imager design [26] that combines the CMOS/CCD or any photo-detector array (PDA) sensor with the CAOS platform. Here the CAOS imager functions as a smart high dynamic range image information sifter that is guided by a raw image data generating CCD/CMOS PDA imager. This paper describes a variety of such novel CAOS camera-based instrument designs suited for a variety of applications. A basic experimental demonstration of the CAOS camera is also presented.

2. THE BASIC CAOS CAMERA

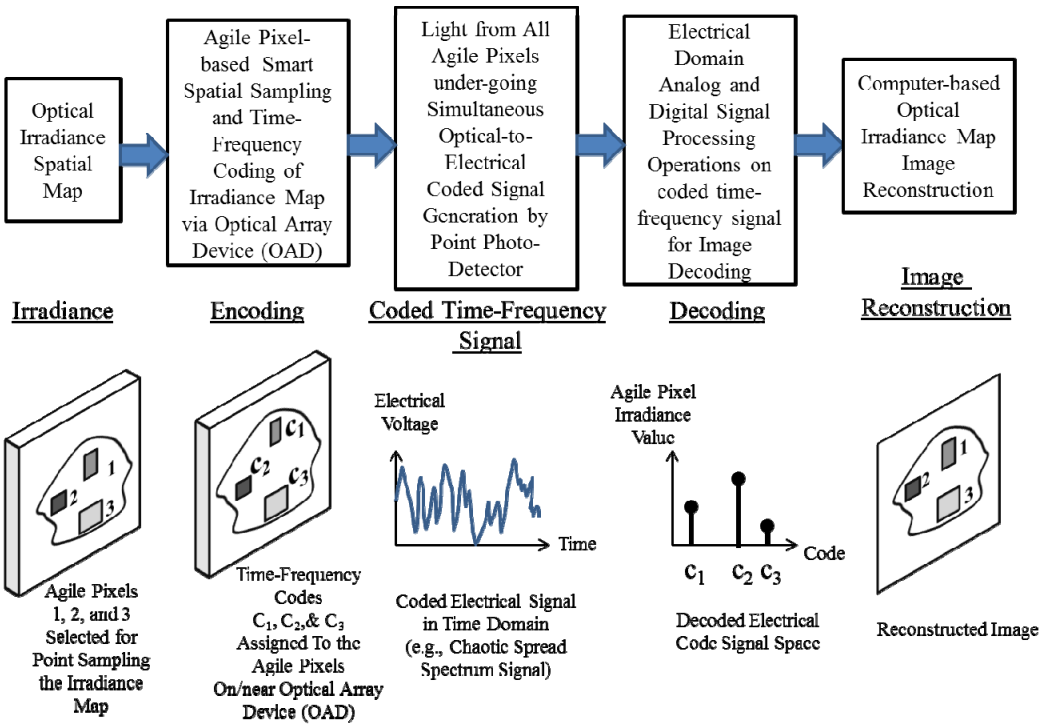

Fig.1. CAOS Imager Signal Flow Chart.

Motivated by modern day advances in RF wireless, optical wired communications and electronic signal processing technologies and using our prior-art SLM-based imager design [6], described is a new imager design called Coded Access Optical Sensor (CAOS) [25] that has the ability to alleviate some of the mentioned prior imager fundamental limitations using a surprisingly simple approach. To elaborate on the signal flow workings of the CAOS

imager, Fig.1 shows a signal flow chart where shown are 3 different sizes, shapes, and positions of the agile pixels labelled as 1, 2, and 3 that are coded with codes c_1, c_2, and c_3, respectively. All the time-frequency coded optical signals engage simultaneously on the PD. This optical analogy is similar to the cell phone scenario where numerous EM signals incident on the RF antenna is equivalent to the many optical agile pixels in the irradiance map incident simultaneously on the point PD. Decoding of agile pixel position based irradiance values is implemented by using the PD generated temporally varying electrical signal and subjecting it to high speed analog and digital electronics-based one Dimensional (1-D) coherent (i.e., electrical phased locked) or incoherent signal processing. With the agile pixel-based irradiance values recovered from what looks like a chaotic RF signal, computer-based non-iterative image (2-D) processing and reconstruction techniques are used to stitch together the 2-D optical irradiance map observed by the CAOS Imager. Do note that the selected sizes, shapes, and locations of the agile pixels within a given sampling time slot should be optimized to extract the desired image features with maximum SNR based on application specific intelligence. The speed of image capture rate can be fast (i.e., >> 60 Hz) given a high speed point PD is used in the imager to simultaneously detect the sampled pixel irradiances in the OAD and one will avail very high speed optoelectronics and microelectronics for CAOS signal coding and decoding. As mentioned, coherent (phase-locked) high sensitivity detection in the electrical domain can also be used for decoding of the agile pixels. In addition, advanced CAOS designs can also use optical field encoding and coherent optical detection and decoding

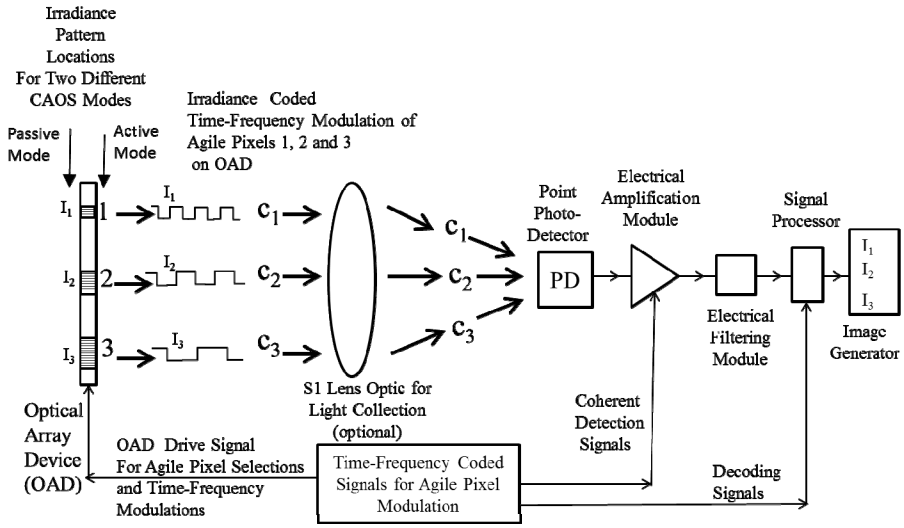

Fig. 2 Basic CAOS Imager Implementation (Side View).

Fig. 2 shows an implementation of the basic CAOS imager that can operate in two modes of imaging. The passive mode of CAOS imager operation occurs when irradiance to be imaged comes from an external radiation source (e.g., star light, laser) and falls on the programmable Two Dimensional (2-D) Optical Array Device (OAD) agile pixels-plane. The active mode of operation occurs when the OAD acts as an internal pixelated radiation source that illuminates the object undergoing imaging. This object can be in the near-field, i.e., placed at or adjacent to the OAD agile pixels-plane (Fig.2 design) or in the far-field where imaging optics is used to project the OAD modulated light onto the object. The agile pixel can operate in different time-frequency coding modes like Frequency Division Multiple Access (FDMA), Code-Division Multiple Access (CDMA), and Time Division Multiple Access (TDMA). CDMA and FDMA will produce spread spectrum RF signals from the point Photo-Detector (PD) while TDMA is the staring-mode operation of the CAOS imager, one agile pixel at a time producing a DC signal per agile pixel position (same as our original DMD-imager). For full impact of the CAOS imager, agile pixel codes should include CDMA, FDMA or mixed CDMA-FDMA codes that produce not only PD signals with a broad RF spectrum (that looks like a chaotic RF signal), but also engages sophisticated Analog (A), Digital (D), and hybrid information coding techniques to provide isolation (e.g., minimum cross-correlation) and robustness amongst time-frequency codes used for OAD pixel coding. It is important to note that CAOS operates on the basis of time-frequency encoded pixel multiplexing and time-frequency decoded pixel de-multiplexing to recover the smart agile pixel sampled image irradiance. So encoding/decoding relies on time-frequency domain signal processing such as correlation in wireless and radar receivers. CAOS does not deploy random spatial

coding of the SLM or spatial correlations and iterative image processing such as in compressive or computational sensing to recover the image.

Compared to prior-art imagers, the CAOS platform instantaneously brings the following unique features to the proposed imager:

(a) Direct use of both photonic domain and electronic domain information processing. This cascading image control architecture forms a serial-parallel high noise rejection processor that enables generation of high SNR images, in particular for high contrast imaging applications.

(b) The agile pixel space-time-frequency characteristics can be programmed to suit the imaging scenario with adaptive control deployed as needed.

(c) Staring mode PDs such as CCD/CMOS sensors naturally produce a photo-detection electrical noise spectrum that is dominant around the DC and lower frequency components. The CAOS imager produces its photo-detected signal at a temporal frequency band that is away from the noisy part of the PD output near DC, thus creating a higher SNR signal for decoding signal processing. All electronics are fundamentally subjected to 1/frequency (f) or 1/f noise. By having the output signal frequency band for the PD in the CAOS imager away from DC, the 1/f noise in the signal processing electronics chain is also lower as f can be from tens of Hertz to many GHz.

(d) After photo-detection, electrical domain coherent detection such as with electronic mixing plus phased locked amplification and filtering can provide detection of extremely weak signals buried in noise enabling high contrast imaging. The CAOS imager exploits this coherent detection and processing feature in the robust electrical domain versus a vibration/optical phase sensitive optical domain of traditional optical interferometry.

(e) Advanced CAOS designs can also use optical field encoding and coherent optical detection and decoding, much like today's coherent fiber-optic data communication systems, thanks to current CMOS electronic chip technology that can provide D-to-A & A-to-D converter speeds up-to 90 Giga-Samples/second that are integrated with DSP processors containing near 100 million gates [27-28].

(f) The spatial imaging resolution of the CAOS imager is determined by the size of the agile pixel selected for time-frequency coded modulation on the OAD and not by the optical quality of the diffraction limited optic S1 when considering near-field imaging. For passive mode of operations, the OAD is a transmissive (or reflective) SLM device. In this case, the smallest size of the time-frequency modulating agile pixel is the smallest size of the programmable pixel in the SLM. Various SLM technologies can be deployed such as using optical MEMS/NEMS, liquid crystals, Multiple Quantum Wells, etc. Optically addressed pixel structure-free SLMs can also be deployed as the OAD. In the case of imager active mode operations, the OAD is a light source array device like a 2-D optical display device, e.g., a 2-D laser array or a 2-D LED array or a fiber-waveguide array coupled light source array. Depending on the OAD technology, in the near future one can even envision a pixel size as small as an atomic radiator, easily beating the diffraction limit for near field imaging.

(g) Because all agile pixel positions and their irradiances on the OAD are coded in time-frequency and decoding of pixel information no longer depends on the optical diffraction limits of the lens optics in the imager, exceptionally low inter-pixel crosstalk levels can be achieved via the electronic signal processing operations even when the pixel sizes are much smaller than the Abbe diffraction limit.

(h) The optical signal incident on the PD as well as the PD generated electrical signal look chaotic and are inherently secure as the image cannot be recovered without the pixel codes needed for decoding at the receiver.

(i) The CAOS platform is extendable to Three Dimensional (3-D) imaging techniques including light sheet [2], confocal [29], and wavelength diversity-based methods [30], by also applying time-frequency coding to pixels in the third spatial dimension. In addition, the CAOS imager can be combined with classical 2-D CCD/CMOS-based imagers to interrogate sub-2-D image zones in the full 2-D image space where sub-critical data must be extracted from the image scene [26].

(j) Because a high speed point PD is used for optical-to-electrical conversion with imaged pixel positions simultaneously detected and have coding with significantly high electrical frequency content (i.e., short sampling period in the time domain), fast 3D imaged objection motion effects can be captured using electrical

frequency-based Doppler signal processing and Time-of-Flight (TOF) light-based CW and pulsed radar techniques.

3. FIRST EXPERIMENTAL DEMONSTRATION OF THE CAOS CAMERA

For a first demonstration of the basics of the CAOS imager, we choose to image the 2-D irradiance map of a CW visible laser beam that showcases both extreme brightness and dim light zones. The CAOS imager was set-up in the non-coherent electrical detection mode using a Texas Instruments (TI) DMD as the OAD (see Fig.3(d)). As shown in Fig.3, we generate the full image of the incident laser beam irradiance by operating the CAOS imager agile pixel in a hybrid FDMA plus TDMA mode by scanning 3 agile pixels in a raster format line scan and collecting the PD data for Fast Fourier-Transform (FFT) processing and agile pixel irradiance decoding. Three agile pixels at a time at the DMD chip plane are coded with on/off modulations of $f_1 = 80.1$ Hz, $f_2 = 133.4$ Hz, and $f_3 = 200.2$ Hz resulting from the two-tilt state nature of the DMD chip micromirrors.

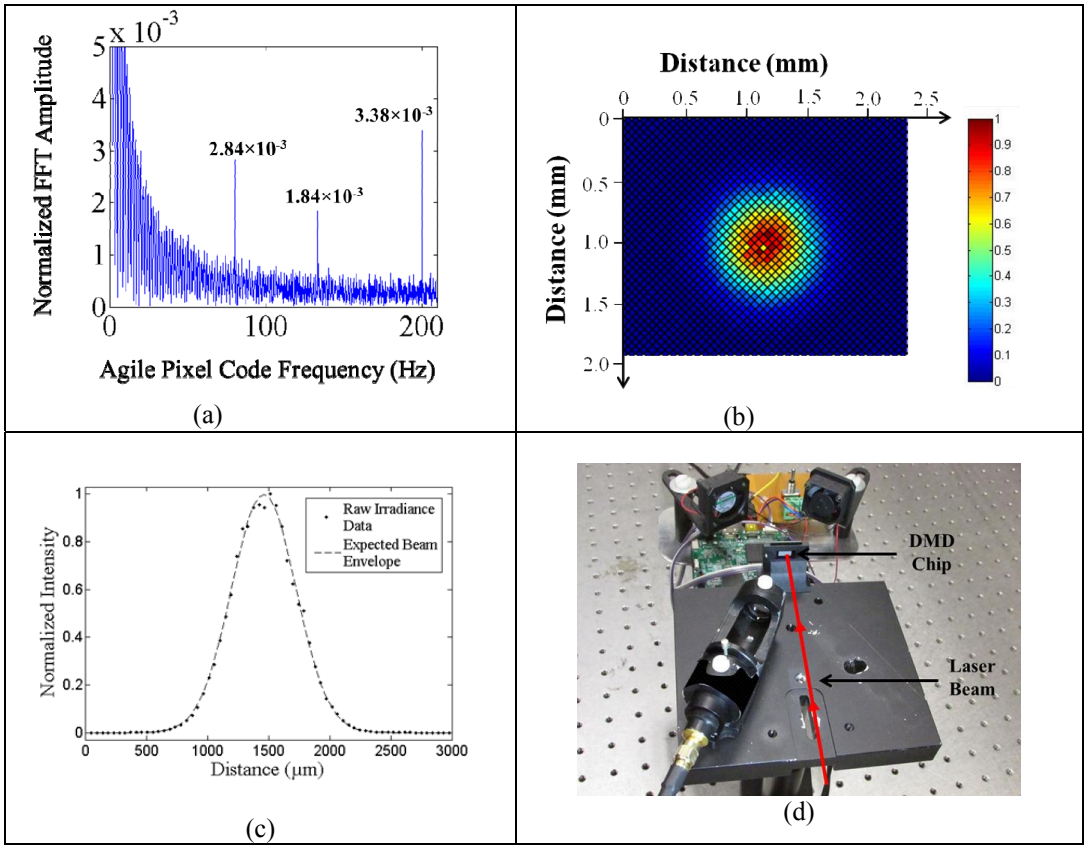

Fig.3(a) FFT signal processing decoding of the three micromirrors agile pixel irradiances I_1, I_2, and I_3 that are proportional to the normalized spectral values computed by the FFT operation. Fig.3(b) shows the 2-D irradiance of 2160 agile pixels data (60 × 36 = 2160) from the experimental CAOS imager demonstrating a 77 dB SNR with SNR in dB = 20 log (I_{max}/I_{noise}).(c) Comparison of central cross-section data of the CAOS imager acquired laser beam image (dots) vs. laser manufacturer provided theoretically expected Gaussian beam envelope (dashed line). (d) CAOS Imager Optical Experimental setup. [25]

Fig.3(a) shows the FFT signal processing decoding of the three agile pixel irradiances I_1, I_2, and I_3 at the DMD chip. To generate preliminary CAOS image data giving a 77 dB SNR, the imager operated with a total of 2160 agile pixels time modulating via FDMA coding in sets of three with each set modulating for 6.24 seconds followed by a 14 seconds delay before the next set modulated to ensure synchronization between PC, μC and LCr DMD board with each

agile pixel being 6 x 6 micromirrors, with a micromirror with 7.64 μm sides. Compared to our previous non-time coded starring mode DMD agile pixel imager, the electrical SNR of the CAOS imager has improved by 5 orders of magnitude (>55 dB). Using the acquired CAOS imager-based irradiance 2-D spatial beam map shown in Fig.3(c) and 2-D Gaussian fitting in MATLAB , obtained are $1/e^2$ laser beam waists radii of w_x = 526.0 μm and w_y = 530.1 μm. In comparison, using Gaussian laser beam propagation theory and the laser manufacturer data sheet 325 μm minimum beam waist radius and 67.5 cm beam travel distance to DMD, one gets $w_x = w_y$ = 529.9 μm. This manufacturer specified beam radius value is within 0.75% error (i.e., 100% ×(529.9-526)/529.9) of the CAOS imager Fig.3(c) data provided 2-D Gaussian fitting measurement. The speed of imaging of this 1st CAOS imager is limited at present because of the non-custom and low cost nature of the components that are designed for low cost low speed DMD Lightcrafter board human viewing display application. Presently, the more costly TI DMD advanced kit can provide frame rates reaching 30 KHz with individual micro-mirror reset times of near 15 microseconds.

4. CAOS CAMERA INSTRUMENT DESIGNS AND APPLICATIONS

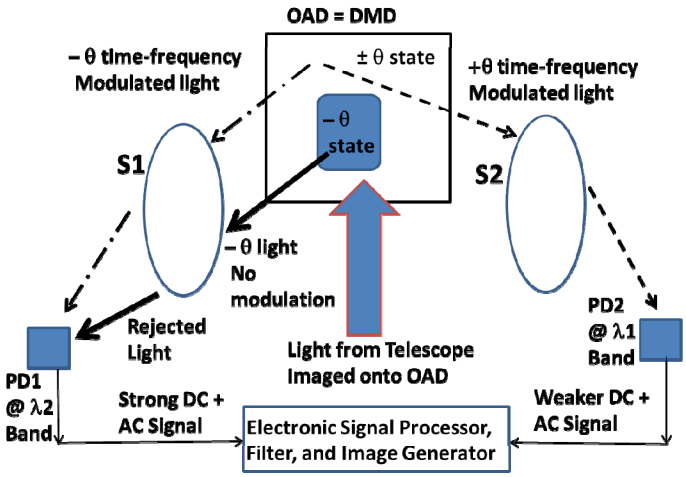

Fig.4 Passive CAOS coronagraph for astronomical imaging.

The CAOS platform can be used to design a variety of instruments for applications in science and industry. For example, a powerful CAOS-based coronagraph can be designed for direct exoplanet imaging [31-34] where scenes require extreme (>10^4) contrast sensing, e.g., Visible band (>10^9 contrast) and IR 1.65 and 2.1 microns (>10^7 contrast). The contrast power of the proposed passive CAOS coronagraph comes from simultaneously using pixel-controlled optical filtering combined with electronic filtering including electronic coherent signal processing and filtering. In effect, a cascade of filters operates on the light irradiance data to yield high contrast imaging. The Fig.4 CAOS coronagraph design using a DMD as the OAD can operate simultaneously with two different band point PDs enabling simultaneous multispectral band imaging. Adding dichroic beam splitters with additional wavelength specific PD (this includes bolometers, APDs, PMTs) plus optical attenuators before PDs can enhance performances in terms of spectral detection, dynamic range, and sensitivity. The bright unwanted zone in the image scene is given a time static –θ micromirror state in the DMD pixel set while the desired image zone pixel set is time-frequency modulated using both ±θ digital tilt states of the DMD. The rejected light shows up as a strong DC electrical signal via PD1.Lenses S1 and S2 transfer light from the OAD plane to the PDs. The desired time-frequency coded signals provided by both PD1 and PD2 show up as AC electrical signals that undergo electronic signal processing, filtering (including DC signal blocking), and image reconstruction to produce the desired high contrast image. Compared to prior coronagraphs, CAOS opens up the possibility of full image scene pixel programmability and spectral flexibility by using both spatial domain optical filtering plus time domain electronic filtering that can lead to potentially higher contrast (from 80 dB to 190 dB electrical dynamic range) highly adaptive astronomical imaging telescopes that can look deeper into the cosmos searching for fundamental physics answers such as via dark matter and dark energy detection. CAOS broadband imaging capability also allows high dynamic range detection of emission spectra for planetary body signature mapping.

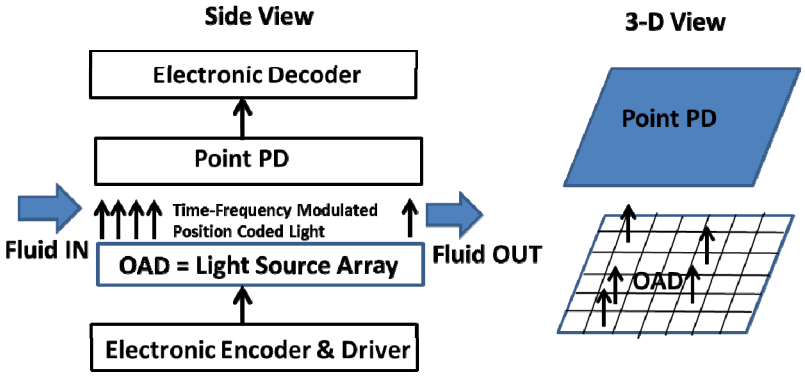

Fig.5. Active CAOS -Near Field Lensless Cube Microscope.

Imaging within the marine ecosystem is a challenging task given the fluidic environment with dark low light conditions including scattering effects [35-36] . Active CAOS uses a Light Source Array (LSA) to provide an active smart lighting position-coded mechanism to extract target imaging information from a fluidic environment. Fig.5 shows an ultra-compact CAOS imager cube design to be developed for microscopic marine fluidic samples. The lensless design essentially consists of five chips stacked together forming a cube with the gap between the OAD chip and point PD forming the fluidic channel to introduce the samples undergoing imaging. The gap of the fluidic channel is short to ensure optical near field sampling conditions and the spatial resolution of the imager is essentially determined by the active area of the light emitters. Via control of light power at each sampling pixel location, it is expected that higher contrast fluidic imaging will be possible. With LSA devices forming arrays of nano-size emitters (e.g., using custom designed demonstration devices) [38-39], nano-scale near-field imaging resolutions are expected without the use of fluorescence, recently cited as "*the holy grail of superresolution microscopy is to break free from the shackles of fluorescent labels*" [2].

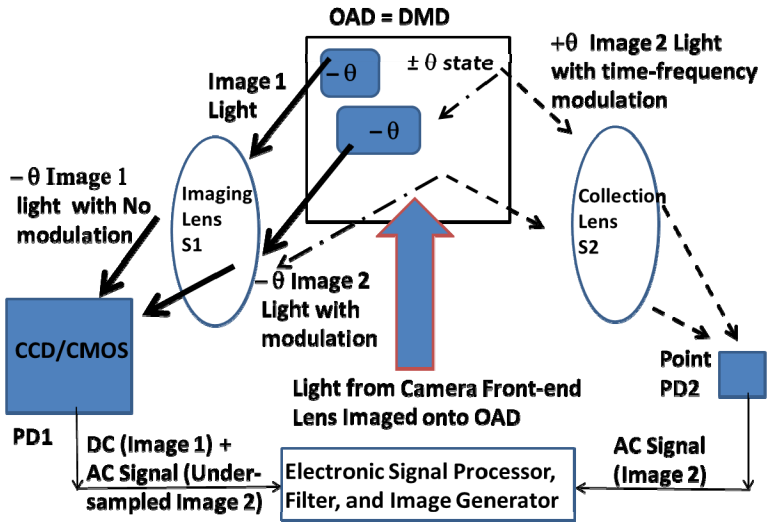

Fig.6 Passive CAOS- CCD/CMOS Dual Imager.

Another application for the CAOS camera is far-field 2D underwater (UW) marine ecosystem imaging [37] where a bright target light spot (e.g., search light) is used to illuminate the marine region of interest. Fig.6 shows a passive CAOS-CCD/CMOS dual imager design used to extract two different light level images called Image 1 (e.g., low

light image) and Image 2 (e.g., bright image) with the two images combined in software to create one high contrast image. Image 1 is created using a classic CCD/CMOS sensor as PD1 while PD2 is a higher speed point PD that has the bandwidth to sample the time-frequency modulated Image 2 select pixels in the OAD. Scheimpflug imaging condition is maintained between OAD and PD1 using lens S1. PD1 produces a DC signal carrying the Image 1 data and an under-time sampled AC signal that carries some Image 2 data. Using electronic filtering to remove the AC component, PD1 can produce the Image 1 signal. Using light collection lens S2, PD2 produces a CAOS encoded AC signal with the Image 2 select pixel data. Thus, a high contrast hybrid design imager is formed using a dual-camera system based on CAOS as well as CCD/CMOS sensor that engages the best features of both sensor technologies. Note that variable optical attenuators can be engaged in both optical paths between the DMD and the photo-detectors to acquire unsaturated photo-detected data to further enhance the camera dynamic range using electronic post-processing. In addition, programmable optical color filters, variable apertures, and polarizers can also be added at the entrance of the camera and/or between the DMD and PD1/PD2, giving further functionality to the CAOS-CCD/CMOS Dual Imager.

The Figure 6 Passive CAOS-CCD/CMOS Dual Imager is also suited for several industrial inspection and accident prevention imaging scenarios involving high optical contrast scenarios and/or high speed remote sensing and machine vision. These include laser-based welding, surface vibrometry, flows capture, ablation and cutting, non-destructive 2-D and 3-D measurements of machine parts, and accident prevention mobile platform night vision imaging using for example NIR laser (0.75 to 1.4 micron) for target illumination. Specific health and safety machine vision applications include mobile platforms where blinding lights can impair machine vision used to control platform maneuvers such as for aircrafts, cars, boats, cranes, ships, submarines, helicopters, and UAVs/drones.

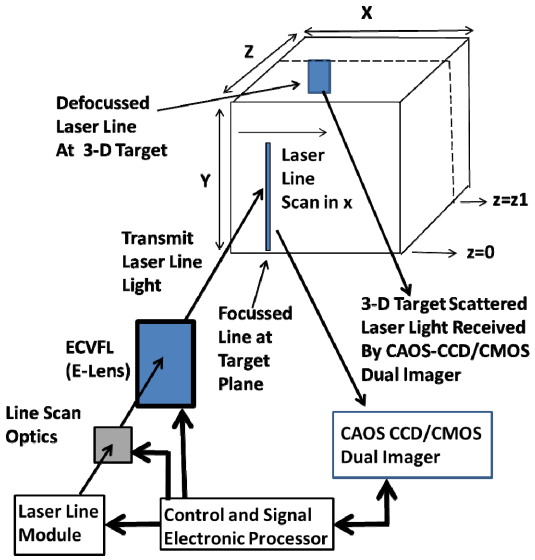

Fig.7. CAOS plus Laser-Electronic Lens-based 3-D Imager.

The CAOS platform can engage with the prior-art laser-driven electronic lens shape sensor [40-45] to design powerful machine vision systems for industrial 3-D parts inspection. As shown in Fig.7, a laser line after passing through an E-lens falls on the 3-D target. A CAOS CCD/CMOS dual imager is used to view the bright laser light scattered from the 3-D target. As shown in Fig.7, depending on the target depth plane (along z-direction), the line thickness (along x-direction) seen by the dual imager is different. By sweeping the E-lens focal length, the observed laser line along different y-directions of the target will produce in-focus laser lines for a different E-lens focal length. By noting these highly focussed line widths and their corresponding E-lens focal lengths, the depth of the target for the different y-direction locations at a given x-direction scan position can be computed using image processing algorithms. Scan optics moves the laser line in the x-direction so the depth measuring process along y-direction for a given x-scan can be repeated over the full x-y field-of-view of the dual imager. Because 3-D reconstruction is based on direct laser-based sampling of the target with the brightly focussed line versus a regular unconditioned expanding laser beam of lower brightness, a best spatial resolution with higher contrast imaging can be achieved. An optimized wavelength bright laser

line can be used with the Fig.7 3-D imager as the CAOS-CCD/CMOS dual imager can handle bright light conditions. In addition, when using the CAOS imager for high speed light detection, TOF techniques can be availed in the system.

Far Field 3D Imaging of Coral is another challenging application in marine ecosystem studies. Monitoring of marine ecosystems such as coral is vital for the survival of the larger ecosystem surrounding the water-sustained habitats of human, marine and animal species. The ability to realize powerful yet low cost optical 2-D and 3-D imagers via CAOS can allow larger scale mapping and frequent, including some real-time high speed monitoring of these underwater micro and macro environments leading to better government planning to preserve and enhance these vital and economically important ecosystems [46-47].

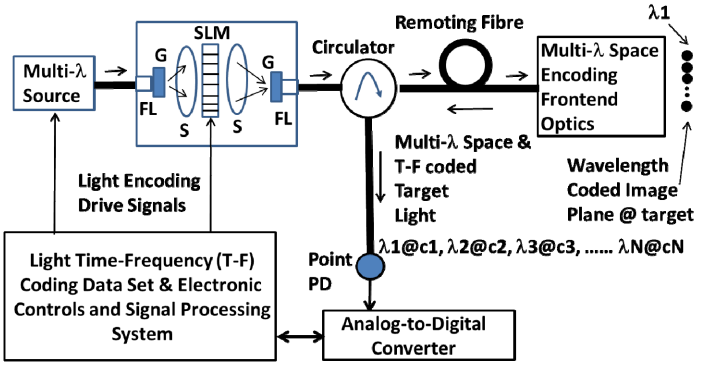

G: Grating; FL: Fibre Lens; S: Lens; SLM: Spatial Light Modulator; PD: Photo-Detector
c1, c2, c3, etc are time-frequency codes for wavelengths λ1, λ2, λ3,etc, respectively.

Fig.8. CAOS-WMOS platform forming the CAOS wavelength coded fibre remoted 2-D and 3-D imager. WMOS: Wavelength Multiplexed Optical Scanner.

As shown in Fig.8, the CAOS platform can merge with a wavelength coded imager [48-53] to design a powerful machine vision system that is fibre remoted and allows endoscopic imaging of hard to access zones. Using the Single Mode Fiber (SMF) with ultra-compact micro-optics in the imager front-end, sizes of under 0.5 mm diameter are expected from this task. Note that the frontend is all-passive with no electrical connections/components, although adding of an E-lens in this frontend would allow 3-D confocal imaging. In an alternate design, direct temporal modulation of the multi-λ source module along with CAOS image plane coding can allow the use of TOF light-based CW and pulsed radar techniques to enable 3-D imaging, i.e. transverse image via CAOS and on-axis depth information via TOF processing. The imager is optically powered by a multi-wavelength optical source (e.g., laser array, broadband diode, ultrafast short pulse laser) that has the option to be electrically driven such that each wavelength can be time-frequency coded for CAOS operations. Light from this broadband source enters a fiber-coupled array-modulator such as an SLM-based modulator that can provide time-frequency coding to the different wavelengths if the optical broadband source is not directly modulated for CAOS imaging coding. The CAOS time-frequency coded multiwavelength light passes through a fibre circulator to enter the remoting fibre that terminates in the wavelength dispersive frontend that physically separates the wavelengths to different locations in the spatial scanning zone. Depending on the Dispersive optics used, both 1-D and 2-D grid independent wavelength coded points can be generated in the optical sampling plane. Common dispersion optic components are a Dixon grating, Virtual Phased Array (VPA) grating, Photonic Crystal Prism, silicon photonic waveguide grating coupler, etc. For example, one can use two independent crossed gratings to generate 2-D wavelength coded points in 2-D space or one can deploy multiple volume gratings stored in a 3-D holographic storage material to generate wavelength encoded points in 2-D space. [53-58]. Depending on the field application, the required optical frontend design can be optimized for the fibre-remoted CAOS-WMOS imager. Target reflected light at each wavelength location in the sampling grid returns via the dispersive optics into the SMF and travels via the circulator and optional optical amplifier to the high speed PD. A powerful feature of this imager is the double coding process of each sample pixel location at the target plane. In other words, each sample pixel has a different wavelength code creating optical isolation at the sampling grid plus each wavelength also has its own CAOS time-frequency code that allows electrical isolation between the sampled pixels to enable spatial image decoding via electronic signal processing. The PD signal is digitized by the A-to-D converter and fed to the signal processor. For remoted marine life sampling, the Fig.8 CAOS-

WMOS platform forms a remoting probe that can be used for microscopy of live Coral as well as other microscopic marine organisms and structures. The same probe can also be used in medical imaging applications.

An alternate operational mode and design of a CAOS-WMOS imager is to deploy the CAOS mode to encode light along one dimension of the sample plane (e.g., y-direction with N pixels) while use W-MOS M-wavelength encoding of light along the orthogonal dimension (e.g., x-direction with M-pixels) of the illuminated sample. In this case, a high dispersion fiber needs to be engaged with the sample collected light before it reaches the point-PD so one can separate the M different wavelengths in the time domain via electronic signal processing to recover the x-direction M pixels image data tied to each wavelength. Appropriate lens optics needs to be used to spread the multi-wavelength light along the y-direction so a high speed 1-D N-pixel SLM (along the y-direction) can imprint N different CAOS time-frequency codes on the broadband light corresponding to N-different y-direction pixels illuminating the x-y N x M pixels sample plane. In effect, CAOS encodes the y-direction pixels for each wavelength and W-MOS encodes the x-direction pixels. Such an arrangement can be useful for certain imaging application scenarios. Furthermore, if the use of a high dispersion fiber and its high speed electronics is not suited for a particular application, parallel processing/detection of the M-wavelengths is possible using 1-D dispersive optic (e.g., grating) combined with a 1-D M-pixel PD array. Here each PD in the PD array must electronically decode the CAOS encoded N-pixels for its specific wavelength.

5. CONCLUSION

CCD-based imaging systems arrived in the late-60s [59-63] while a quarter of a century later in the mid 90s, CMOS (also called APS-Active Pixel Sensor)-based imagers made their entry into science and industry [64]. Now the CAOS platform has arrived [24-25] to realize EM radiation-based imaging systems that when combined with prior-art sensors can realize exceptional performance imaging systems for diverse applications in science and industry. This paper has summarized the CAOS platform vision and its example novel imager designs that can create impact across fields of astronomy, machine vision, undersea observations and marine science, and medical imaging. Looking at the past, an observation is that every quarter of a century, a new powerful imager technology is ushered in by humankind. It is hoped that CAOS will indeed create the considerable impact outlined in this paper.

6. REFERENCES

1. N. Waltham, “CCD and CMOS sensors: Observing Photons in Space,” Springer New York, 2013.
2. S. Weisenburgera and Vahid Sandoghdar, “Light microscopy: an ongoing contemporary revolution,” Contemporary Physics, Vol. 2, pp.123-143, Taylor Francis, 2015. (Review Paper on prior-art Imaging)
3. E. Rittweger, K. Y. Han, S. E. Irvine, C. Eggeling, and S. W. Hell, “STED microscopy reveals crystal colour centres with nanometric resolution,” Nature Photonics 3, 144-147, 2009.
4. B. Cremers, et al., “A 5 megapixel, 1000 fps CMOS image sensor with high dynamic range and 14-bit A/D converters," International Image Sensor Workshop, Snowbird Resort, UT, USA, 2013.
5. K. Kitamura, et.al., “A 33 Mpixel, 120 fps CMOS Image Sensor for UDTV Application with Two-stage Column-Parallel Cyclic ADCs,” IISW, 2011.
6. S. Sumriddetchkajorn and N. A. Riza, “Micro-electro-mechanical system-based digitally controlled optical beam profiler,” Applied Optics, 41, 18, 3506-3510, 2002.
7. N. A. Riza and M. J. Mughal, "Optical Power Independent Optical Beam Profiler," Optical Engineering, 43, 4, April 2004.
8. N. A. Riza and F. N. Ghauri, “Super Resolution Hybrid Analog–Digital Optical Beam Profiler Using Digital Micromirror Device,” IEEE Photonics Technology Letters, vol. 17, no. 7, 2005.
9. M. Gentili and N. A. Riza, “Wide Aperture No Moving Parts Optical Beam Profiler Using Liquid Crystal Displays,” Applied Optics, Vol.46, pp.506-512, 2007.
10. M. Sheikh and N. A. Riza, “Demonstration of Pinhole Laser Beam Profiling using a Digital Micromirror Device,” IEEE Photon. Tech. Lett, Vol.21, May 15, 2009.
11. N. A. Riza, S. A. Reza and P. J. Marraccini, “Digital micro-mirror device-based broadband optical image sensor for robust imaging applications,” Optics Communications 284, 1, 2011.

12. N. A. Riza, P. J. Marraccini, and Cody Baxley, " Data Efficient Digital Micromirror Device-Based Image Edge Detection Sensor using Space-Time Processing," Vol.12, No.5, p.1043-1047, May 2012.
13. M. J. Amin, J. P. La Torre and N. A. Riza, "Embedded Optics and Electronics Single Digital Micromirror Device-based Agile Pixel Broadband Imager and Spectrum Analyser for Laser Beam Hotspot Detection," Applied Optics, 54, 3547–3559, 2015.
14. A. S. Selivanov, V. N. Govorov, A. S. Titov, and V. P. Chemodanov, "Lunar Station Television Camera," (Reilly Translations, transl.): NASA CR-97884, 1968.
15. F. O. Huck and J. J. Lambiotte, "A Performance Analysis of the Optical-Mechanical Scanner as an Imaging System for Planetary Landers," NASA TN D-5552, Dec.1969.
16. D. Takhar, J. N. Laska, M. B. Wakin, M. F. Duarte, D. Baron, S. Sarvotham, K. F. Kelly, R. G. Baraniuk, "A New Compressive Imaging Camera Architecture using Optical-Domain Compression," SPIE-IS&T Proc., 6065, 606509-1, 2006.
17. J. H. Shapiro, "Computational ghost imaging," Physical Review A, 78, 061802(R), 2008.
18. O. Katz, Y. Bromberg, Y. Silberberg, "Compressive ghost imaging," Applied Physics Letters 95, 131110, 2009.
19. M. J. E. Golay, "Multi-slit spectrometry," J. Opt. Soc. Am. 39, 437–444, 1949.
20. P. Gottlieb, "A television scanning scheme for a detector-noise limited system," IEEE Trans. Infom. Theory 14, 428–433, 1968.
21. E. E. Fenimore, "Coded aperture imaging: predicted performance of uniformly redundant arrays," Appl. Optics **17**, 3562–3570, 1978.
22. W. T. Cathey, and E. R. Dowski, "New paradigm for imaging systems," Appl. Optics 41, 6080–6092, 2002.
23. N. A. Riza and M. A. Arain, "Code multiplexed optical scanner," Applied Optics, IP, Vo.42, No.8, March 10, 2003.
24. N. A. Riza, Patent Pending.
25. N. A. Riza, M. J. Amin and J. P. La Torre, "Coded Access Optical Sensor (CAOS) Imager," Journal of the European Optical Society (JEOS) Rapid Publications, Vol. 10, 15021, April 19, 2015. (open access on-line Journal of EOS www.jeos.org)
26. N. A. Riza, Compressive optical display and imager, US Patent 8783874 B1, July 22, 2014.
27. P. J. Winzer, "Scaling Optical fiber networks: challenges and solutions, OSA OPN Magazine, 26, no. 3, 28-35, March 2015.
28. C. Laperle and M. O'Sullivan, "Advances in high-speed DACs, ADCs, and DSP for optical coherent transceivers," IEEE/OSA J. Lightw. Technol 32.4, 629-643, 2014.
29. J. Pawley, "Handbook of biological confocal microscopy," Springer, 2010.
30. N. A. Riza, "Multiplexed Optical Scanner Technology," US Patent 6,687,036, 2004.
31. B. Macintosh, et. al., "First light of the gemini planet imager," Proceedings of the National Academy of Sciences 111.35, 12661-12666, 2014.
32. M. Chun, et al. "Performance of the near-infrared coronagraphic imager on Gemini-South," arXiv preprint arXiv:0809.3017 , 2008.
33. J. R. Males, et.al., "High contrast imaging of an exoplanet with the Magellan VisAO Camera," Proceedings of the International Astronomical Union8.S299 46-47, 2013.
34. A. Sivaramakrishnan, et al., "Gemini Planet Imager coronagraph testbed results," SPIE Astronomical Telescopes+ Instrumentation. International Society for Optics and Photonics, 2010.
35. K. Ku, R. Bradbeer, and K. Lam, "An underwater camera and instrumentation system for monitoring the undersea environment,"Mechatronics and Machine Vision in Practice. Springer Berlin Heidelberg, 2008.
36. H. Singh, et al., "Imaging coral I: Imaging coral habitats with the SeaBED AUV," Subsurface Sensing Technologies and Applications 5.1, Springer, 25-42, 2004.
37. E. G. Reynaud, Editor, Imaging Marine Life: Macrophotography and Microscopy Approaches for Marine Biology, Wiley-Blackwell, Dec., 2013
38. P. Yang, R. Yan, and M. Fardy, "Semiconductor Nanowire: What's Next?," Nano Letters, 10, 2010.

39. M-L Kuo, Y-S Kim, M-L Hsieh, and S-Y Lin, "Efficient and Directed Nano-LED Emission by a Complete Elimination of Transverse-Electric Guided Modes," Nano Letters, 11, 2011

40. N. A. Riza and S. A. Reza, "Smart Agile Lens Remote Optical Sensor for Three Dimensional Object Shape Measurements," Applied Optics, Vol. 49, No. 8, March 10, 2010.

41. M. J. Amin and N. A. Riza, "Smart laser scanning sampling head design for image acquisition applications," Applied Optics, 52, 20, 10 July 2013.

42. N. A. Riza and M. J. Amin, "Multi-Image Acquisition based Distance Sensor using Agile Laser Spot Beam Targeting," Applied Optics, 53(25), 5807-5814, 2014.

43. N. A. Riza, Hybrid optical distance sensor, USA Patent 8,107,056, Jan.31, 2012.

44. N. A. Riza and F. Perez, Spatially Smart Optical Sensing and Scanning, USA Patent 8,213,022, July 3, 2012.

45. N. A. Riza and H. Foroosh, Hybrid differential optical sensing imager, USA Patent 8,587,686, Nov.19, 2013.

46. B. Beall, et. al., "3D reconstruction of underwater structures," Intelligent Robots and Systems (IROS), 2010 IEEE/RSJ International Conference on. Intelligent Robots and Systems October 18-22, 2010, Taipei, Taiwan, 2010.

47. B. J. Veal, et al., "A comparative study of methods for surface area and three-dimensional shape measurement of coral skeletons," Limnology and Oceanography: Methods 8.5, 241-253, 2010.

48. N. A. Riza, "Wavelength Switched Fiber-Optically Controlled Ultrasonic Intracavity Probes," IEEE LEOS Ann. Mtg. Digest, pp.31-36, Boston, 1996.

49. G. J. Tearney, R. H. Webb, and B. E. Bouma, "Spectrally encoded confocal microscopy," *Optics letters*, Vol.23, No.15, pp. 1152-1154, 1998.

50. N. A. Riza and Y. Huang, "High Speed Optical Scanner for Multi-Dimensional Beam Pointing and Acquisition," IEEE-LEOS Annual Meeting Conf. Proc., San Francisco, CA, Nov. 1999.

51. Z. Yaqoob, A. A. Rizvi and N. A. Riza, "Free-space wavelength multiplexed optical scanner," Applied Optics, 40(35), 6425-6438, Dec. 10, 2001.

52. Z. Yaqoob, and N. A. Riza, "High-speed scanning wavelength multiplexed fiber-optic sensors for biomedicine," Proc. IEEE Sensors Conf., 1, 325–330, 2002.

53. K. Goda, K. K. Tsia, and B. Jalali, "Amplified dispersive Fourier-transform imaging for ultrafast displacement sensing and barcode reading," Appl. Phys. Lett. 93(13), 131109 (2008).

54. M. Shiraski, "Large angular dispersion by a virtually imaged phased array and its application to a wavelength demultiplexer," *Optics letters*, Vol. 21, No.5, pp 366-368, 1996.

55. Z. Yaqoob, M. A. Arain, and N. A. Riza, "High-speed two-dimensional laser scanner based on Bragg gratings stored in photothermorefractive glass," Applied Optics, Vol. 42, no. 26, pp.5251-5262, 2003.

56. T. Chan, E. Myslivets, and J. E. Ford, "2-Dimensional beamsteering using dispersive deflectors and wavelength tuning," *Optics Express*, Vol.16, no. 19, pp. 14617-14628, 2008.

57. K. Goda, K. K. Tsia, and B. Jalali, "Serial time-encoded amplified imaging for real-time observation of fast dynamic phenomena," Nature, Vol. 458, (7242), pp.1145–1149, 2009.

58. K. K. Tsia, K. Goda, D. Capewell, & B. Jalali, "Performance of serial time-encoded amplified microscope," *Optics Express*, Vol.*18*(10), pp.10016-10028, 2010.

59. G. F. Amelio, M. F. Tompsett, and G. E. Smith, "Experimental verification of the charge coupled device concept," Bell Syst. Tech. J. 49, 593, 1970.

60. W. S. Boyle, and G. E. Smith, "Charge coupled semiconductor devices," Bell Syst. Tech. J. 49, 587, 1970.

61. M. F. Tompsett, Charge transfer imaging devices, US Patent 4085456 A, April 18, 1978 (filing date March 16, 1971).

62. M. F. Tompsett, G. F. Amelio, W. J. Bertram, Jr.; R. R. Buckley, W. J. McNamara, J. C. Mikkelsen, Jr.; D. A. Sealer, “Charge-coupled imaging devices: Experimental results,” IEEE Transactions on Electron Devices, Vol. 18, No.11, pp.992–996, November 1971.

63. W. S. Boyle, and G. E. Smith, “Buried channel charge coupled devices,” U.S. Patent No. 3,792,322, 12 February 1974. Note: 2006 Nobel Prize in Physics awarded to W. S. Boyle, and G. E. Smith.

64. E. R. Fossum, S. Mendis, and S. E. Kemeny, “Active pixel sensor with intra-pixel charge transfer,” U.S. Patent No. 5,471,515, 28 Nov. 1995.